Diagn Interv Radiol 2007; 13:213–216

INTERVENTIONAL RADIOLOGY

CASE REPORT

Emergency embolization of a bleeding renal angiomyolipoma using polyvinyl alcohol particles

Anjumara Bora, Abhijit Soni, Nisha Sainani, Deepak Patkar

ABSTRACT

Angiomyolipomas (AMLs) are hamartomatous lesions consisting of abnormal blood vessels, smooth muscle, and adipose tissue. Bilateral AMLs invariably point to a diagnosis of tuberous sclerosis complex (TSC). The risk of hemorrhage in AML is related to tumor size, growth of the tumor, hypervascularization, presence of aneurysms, and association with TSC. We report a case of a young male who presented with painless hematuria. He was diagnosed with bilateral renal AMLs on ultrasonography and computed tomography. The large bleeding lesions were identified by renal angiography and selectively embolized using polyvinyl alcohol particles. To the best of our knowledge, isolated use of polyvinyl alcohol particles has not been previously reported.

Key words: • *angiomyolipoma* • *tuberous sclerosis* • *renal angiography* • *polyvinyl alcohol*

From the Department of Radiology and MRI (N.S. ✉ *docnisainani@yahoo.co.in*), Dr. Balabhai Nanavati Hospital and Research Center, Mumbai, India.

Received 30 April 2006; revision requested 8 July, 2006; revision received 25 August 2006; accepted 12 September 2006.

Angiomyolipomas (AMLs) are hamartomatous lesions of which 80% are sporadic and 20% are associated with tuberous sclerosis complex (TSC). AMLs are encountered in 60%–80% of patients with TSC. Bilateral AMLs commonly point to the diagnosis of TSC (1). Dysmorphic vessels in AMLs can have microaneurysms or macroaneurysms, which may rupture and bleed, resulting in significant morbidity. Hence, monitoring the growth of AMLs is essential and prophylactic embolization is recommended.

Case report

A 24-year-old male was rushed to the emergency department of our hospital with the sudden onset of painless hematuria and left flank pain. General examination was normal, except for pallor. At the time of initial examination, his pulse was 110/min and blood pressure was 110/70 mmHg. Palpation revealed dull tenderness in the left lumbar region. On micturating, frank red urine with occasional blood clots was observed. The patient was immediately catheterized and bladder washes were given. Transabdominal ultrasonography (US) performed with an HDI 5000 (ATL, Philips, USA) using a convex 2–5 MHz transducer, revealed multiple well-defined hyperechoic lesions of varying dimensions in both kidneys (Fig. 1a–d); the largest being in the left lower pole measuring 5.2 × 6.2 cm (Fig. 1d). There was blurring of the corticomedullary junction at places in the left kidney. No calculus or hydronephrosis was seen. The bladder was partially filled and appeared normal (Fig. 1c). Computed tomography (CT) of the abdomen was scheduled for further evaluation. CT was performed with a 4-slice multidetector scanner (Sensation 4, Siemens, WI, USA). Plain CT images revealed mild swelling of the left kidney. Multiple predominantly hypodense lesions with attenuation values ranging from -50 to -70 Hounsfield units (HU) were seen in both kidneys, suggesting the presence of fat in the lesions (Fig. 2a). Hyperdensities were detected in the left renal pelvis, left upper ureter, and bladder (Fig. 2b–d). On intravenous contrast administration, enhancement of the renal parenchyma was seen with hypodense areas within, which revealed subtle patchy enhancement (Fig. 3). Also noted was the fluid level in the left renal pelvis (Fig. 3). Excretory phase showed opacification of the calyces in the right kidney that appeared to be stretched by a lesion (Fig. 3); however, the left renal pelvis did not opacify (Fig. 3). Non-enhancement of the hyperdensity in the dependant portion of the bladder confirmed the presence of clots within (Fig. 3). CT images were consistent with multiple AMLs of varying size in both kidneys and hemorrhage from the left lower pole AML. Bilateral AMLs invariably point to the diagnosis of TSC; hence, the parents of the patient were queried about his past medical history. They recalled 2 episodes of convulsion, which the patient had suffered at the age of 8 years. CT of the brain

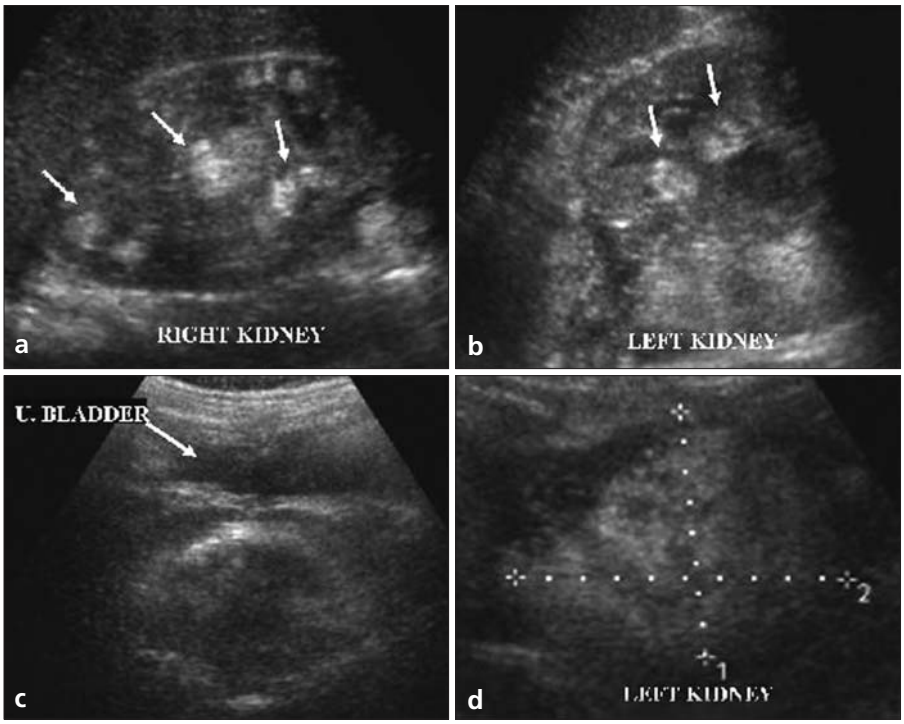

Figure 1. a–d. Ultrasound images **(a–d)** reveal multiple well-defined hyperechoic lesions of varying dimensions in the right **(a)** and left **(b)** kidney *(small white arrows)* with a partially-filled urinary bladder (**c**, *white arrow*). The largest lesion in the lower pole of the left kidney measures 5.2 × 6.2 cm **(d)**.

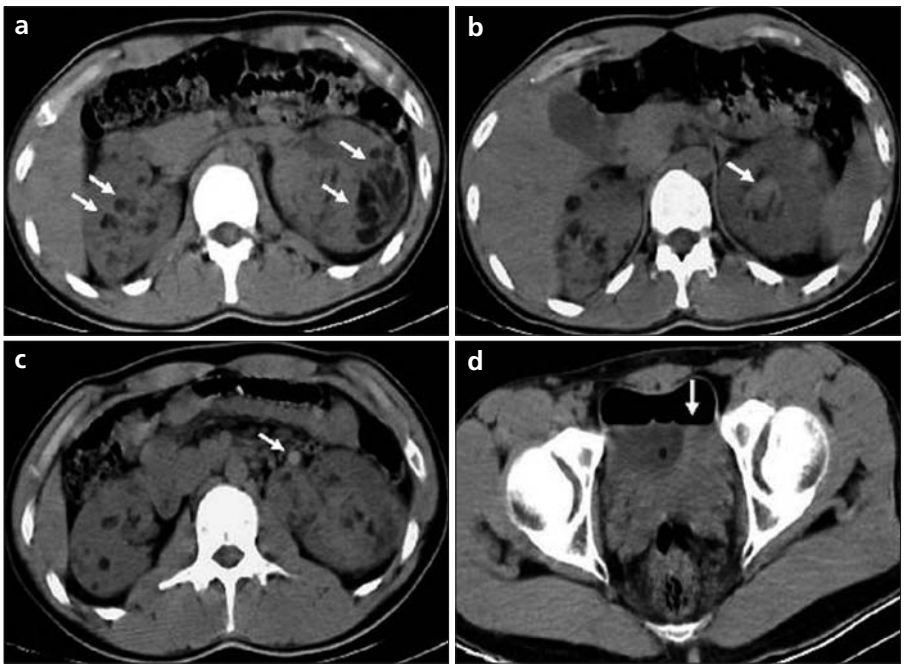

Figure 2. a–d. Plain CT images reveal mild swelling of the left kidney. Multiple hypodense lesions in both kidneys (**a**, *white arrows*). Hyperdensity in the left renal pelvis (**b**, *white arrow*), left upper ureter (**c**, *white arrow*), and bladder (**d**, *white arrow*).

which was subsequently performed revealed subependymal calcifications (Fig. 4).

The patient's condition deteriorated within a span of 8 h, with systolic blood pressure lowering to 80 mmHg and hemoglobin to 8 g/dl. He was maintained on intravenous fluids, blood transfusion, and antibiotics. Cystoscopy revealed oozing of blood from the left ureteral orifice. A double J (DJ) stent was introduced into the left renal pelvis to drain blood clots and prevent deterioration of renal function. Conservative management for 12 h failed to improve the patient's condition. Selective left renal angiogram was performed with a 4 F Headhunter catheter (Johnson & Johnson, Cordis, India) over a 0.025-inch Terumo wire (Radiofocus guidewire, Tokyo, Japan) by an interventional radiologist, and 10 ml of Ultravist (Berlex, USA) contrast (diluted 1:1) was injected. The arterial nephrographic phase showed displacement of vessels in the hilar region due to exophytic tumor growth, with abnormal pooling of contrast in the upper and lower polar regions (Fig. 5). The catheter was advanced to selectively cannulate the lower polar branch, which revealed a densely enhancing 5 × 4 cm lesion that was embolized using polyvinyl alcohol (PVA) particles (250–400 microns) (Ultra Drivalon [Minisys], France) (Fig. 5). The volume of normal renal tissue distal to the lesion was <10%. Branches supplying the upper and mid polar lesions were also selectively cannulated, abnormal vasculature was confirmed, and both lesions were prophylactically embolized, sacrificing a small amount of normal renal parenchyma (Fig. 5). Post-embolization images revealed wedge-shaped defects from embolization, with no significant parenchymal loss (Fig. 5). Approximately 1.5 vials of PVA particles were used to embolize all 3 lesions (each vial contained 0.1 g of polyvinyl formal). This was the dose required for complete occlusion of all 3 vascular lesions, as confirmed with post-embolization images.

Post-embolization, approximately >90% of the residual renal parenchyma was preserved. This was inferred by evaluating pre- and post-embolization arterial nephrographic images. The wedge-shaped area seen on post-embolization images (Fig. 5f) matched the abnormal vascular tumorous area on pre-embolization images (Fig. 5b). Post-embolization syndrome was managed with antipyretics and analgesics. Post-procedure urine was clear and the patient stabilized within a few hours, with a blood pressure of 110/70 mmHg and without support. The patient was discharged on the third postoperative day. At the 1-month follow-up, the DJ stent was removed and he reported no pain or hematuria. He was scheduled for semi-annual surveillance magnetic resonance imaging scans.

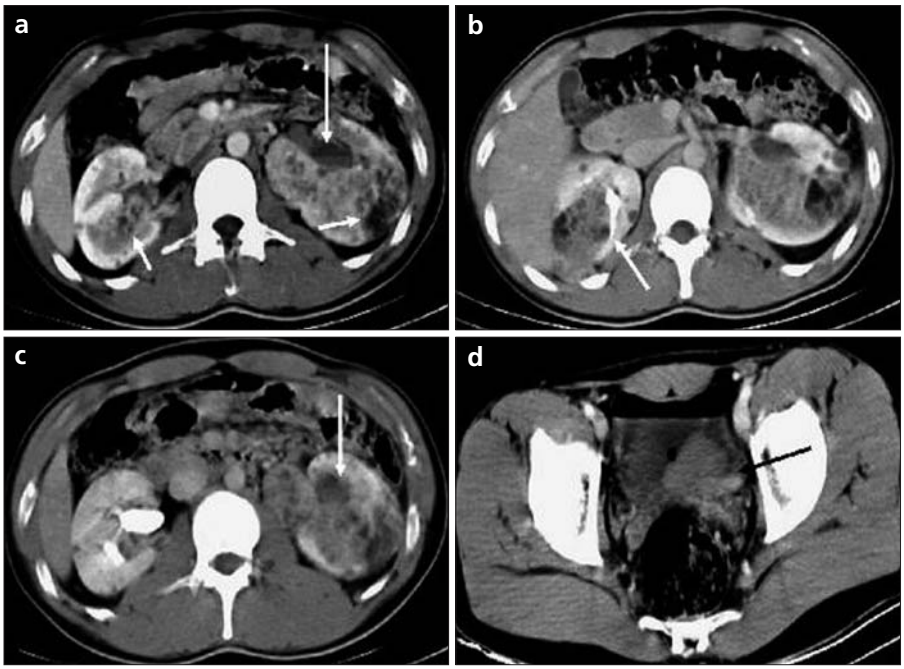

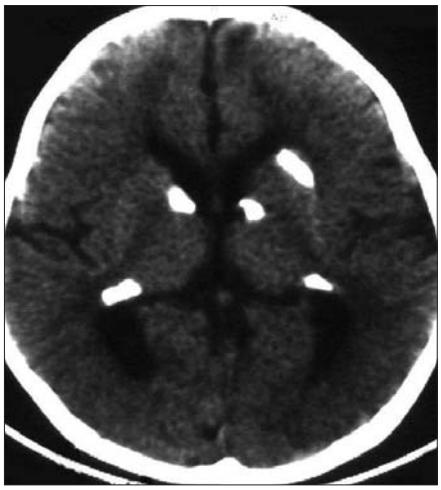

Figure 4. Axial CT section of the brain, revealing subependymal calcifications.

Figure 3. a–d. Contrast-enhanced axial CT images **(a–d)** reveal enhancement of the renal parenchyma and hypodense areas within, revealing subtle patchy enhancement (**a**, *small white arrows*). Fluid level of the left renal pelvis (**a**, *long white arrow*). Opacification of the right renal calyces in the excretory phase, which appear stretched by a lesion (**b**, *long white arrow*). Non-opacification of the left renal pelvis (**c**, *long white arrow*). Non-enhancement of the hyperdensity in the dependent portion of the bladder, suggesting the presence of clots (**d**, *black arrow*).

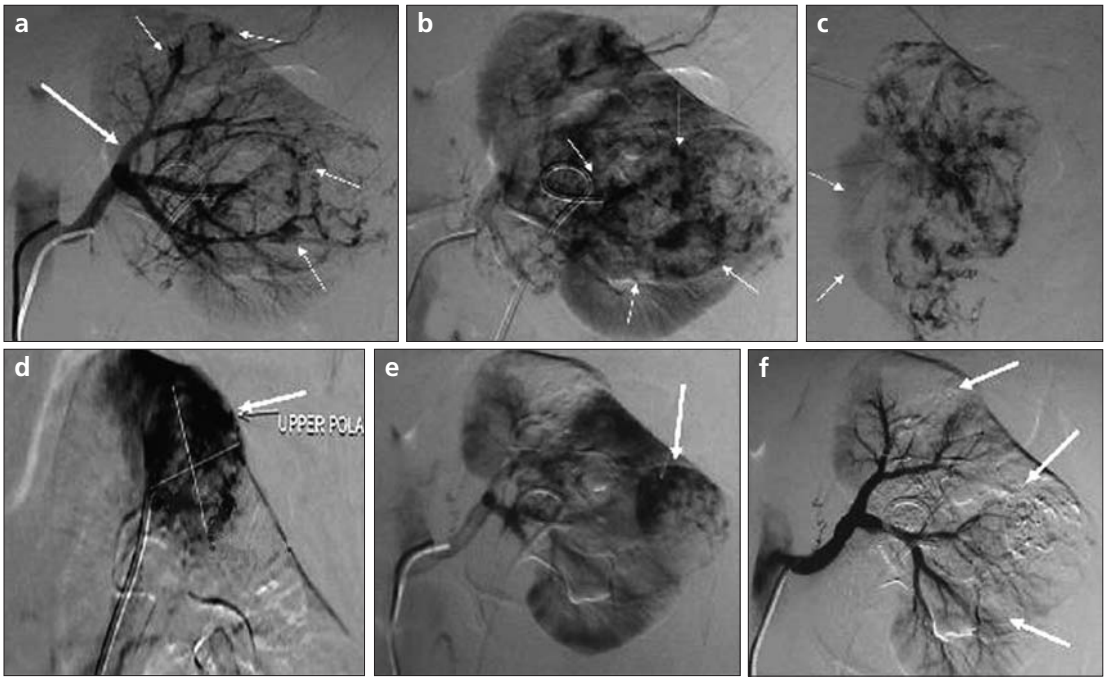

Figure 5. a–f. Selective left renal angiograms. Arterial nephrographic phase (**a**) reveals displaced vessels in the hilar region *(long white arrow)* due to a tumor, with abnormal pooling of contrast in the upper and lower polar regions *(small white arrows).* Angiogram of the lower polar branch (**b**) reveals a densely enhancing 5 × 4-cm lesion *(small white arrows).* Normal renal tissue distal to the lower polar lesion, less than 10% (**c**, *small white arrows).* Upper (**d**, *white arrow)* and middle (**e**, *white arrow)* renal regions reveal abnormal pooling of contrast, suggesting lesions. Post-embolization image (**f**) reveals wedge-shaped defects *(white arrows)* from embolization with no significant parenchymal loss.

Discussion

AMLs are hamartomatous lesions consisting of abnormal blood vessels, smooth muscle, and adipose tissue (1), of which 80% are sporadic and 20% are associated with TSC. AMLs are encountered in 60%–80% of patients with TSC. In these patients AMLs are often large, bilateral, and symptomatic. They develop in childhood and their incidence increases with age (2). Dysmorphic vessels in AMLs can develop microaneurysms or macroaneurysms. These aneurysms may rupture and bleed, resulting in significant morbidity, with pain, loss of renal function, subsequent renal failure, and possibly death, although AMLs do not cause re-

nal failure by themselves (3). Bilateral AMLs invariably point to the diagnosis of TSC, as was seen in our case.

TSC is an autosomal dominant, multi-organ disorder characterized by seizures, mental retardation, and hamartomatous lesions (4). Van Baal et al. followed 20 TSC patients for 5 years and found that in 20% of them the AMLs enlarged, 35% had renal hemorrhage requiring hospitalization, 10% required nephrectomy, and 5% died (5). Serendipitous rapid tumor growth, which occurred exclusively in the 2nd or 3rd decades, with maximal growth of 4 cm per year, was reported in patients with TSC (5, 6). Risk of hemorrhage in AML is related to tumor size (>4 cm), growth curve of the tumor, hypervascularization, presence of aneurysms, and association with TSC; 3 of the above risk factors were present in our patient, resulting in a life-threatening complication of AML (7).

Currently, transarterial embolization (TAE) is the treatment of choice for hemorrhaging in AMLs, because, in contrast to surgery, there is the potential to spare normal renal parenchyma (7). It has been suggested that lesions >4 cm are at greater risk of spontaneous hemorrhage (8); hence, monitoring the degree of AML growth in patients with TSC is important. In our case, TAE was performed to control acute hemorrhaging, and 2 other lesions were embolized prophylactically. Previous studies have reported the use of iodized oil or PVA particles with microembolization coils, or ethanol mixed with iodized oil (Ethiodol) as embolic agents for prophylactic selective trans-arterial embolization of AMLs measuring >4 cm (9, 10). In our case, only PVA particles were used with similar results.

In conclusion, intensive management is generally recommended for AMLs associated with TSC, which are known to have a more aggressive nature than sporadic tumors. Traditional treatment for these large AMLs involves partial or complete nephrectomy. Prophylactic and therapeutic embolization of AMLs is a technically feasible, safe, and minimally invasive procedure. Annual surveillance of TSC patients with AMLs, with abdominal US and CT is essential, as there is a role for prophylactic embolization in the prevention of life threatening hemorrhage (11).

References

1. Hartmut PH, Schwarzkopf G, Henske EP. Renal angiomyolipomas, cysts, and cancer in tuberous sclerosis complex. Semin Pediatr Neurol 1999; 5:269–275.
2. Ewalt DH, Sheffield E, Sparagana SP, Delgado MR, Roach ES. Renal lesion growth in children with tuberous sclerosis complex. J Urol 1998; 160:141–145.
3. Okada RD, Platt MA, Fleishman J. Chronic renal failure in patients with tuberous sclerosis. Association with renal cysts. Nephron 1982; 30:85–88
4. Sampson JR, Harris PC. The molecular genetics of tuberous sclerosis. Hum Mol Genet 1994; 3:1477–80.
5. Van Baal JG, Smits NJ, Keeman JN, Lindhout D, Verhoef S. The evolution of renal angiomyolipomas in patients with tuberous sclerosis. J Urol 1994; 152:35–38.
6. Lemaitre L, Robert Y, Dubrulle F, et al. Renal angiomyolipoma: growth followed up with CT and/or US. Radiology 1995; 197:598–602.
7. Koike H, Muller SC, Hohenfellner R. Management of renal angiomyolipoma: a report of 14 cases and review of the literature—is nonsurgical treatment adequate for this tumor? Eur Urol 1994; 25:183–188.
8. Osterling JE, Fishman EK, Goldman SM, Marshall FF. The management of renal angiomyolipoma. J Urol 1986; 135:1121–1124.
9. Chen P, Racadio J, Bissler J, Donnelly L, Johnson N. Prophylactic embolization of angiomyolipomas in patients with tuberous sclerosis. RSNA 2003 Session: Vascular Interventional Embolization (scientific poster).
10. Kothary N, Soulen MC, Clark TW, et al. Renal angiomyolipoma: long term results after arterial embolization. J Vasc Interv Radiol 2005; 16:45–50.
11. Simmons JL, Hussain SA, Riley P, Wallace DM. Management of renal angiomyolipoma in patients with tuberous sclerosis complex. Oncol Rep 2003; 10:237–241.